JOURNAL OF SOLID STATE CHEMISTRY 68, 11–21 (1987)

A New Classification Scheme to Describe and Predict Structure Types in Pnictide and Silicide Chemistry

JEAN-YVES PIVAN, ROLAND GUÉRIN, AND MARCEL SERGENT

Université de Rennes-Beaulieu, Laboratoire de Chimie Minérale B, Unité Associée au CNRS No. 254, Avenue du Général Leclerc, 35042 Rennes Cédex, France

Received March 19, 1986; in revised form May 15, 1986

Structural homogeneity (symmetry, metal/nonmetal ratio, and atomic coordination) in ternary phosphides of lanthanide and transition metals suggested that the anti-AlB_2, Fe_2P, $Zr_2Fe_{12}P_7$, $Zr_6Ni_{20}P_{13}$, $(La,Ce)_{12}Rh_{30}P_{21}$, $Ho_{20}Ni_{66}P_{43}$, and $La_{18}Rh_{96}P_{51}$ types are members of a structural series. A new method based on triangular units is proposed to describe these structures. The stacking of the units in different modes enables us to describe numerous other structure types, to predict new ones, and to establish a classification scheme in pnictide and silicide chemistry. © 1987 Academic Press, Inc.

I. Introduction

The investigations of ternary lanthanoid–transition metal–metalloid (IIIb, IVb, VIb) systems have resulted in the characterization of numerous ternary compounds, many of them with new structure types. Work on corresponding ternary pnictides is more recent. With nickel or rhodium as transition elements, such materials were synthesized with the following structure types: $ThCr_2Si_2$, $La_6Ni_6P_{17}$, $LaCo_5P_3$, $Zr_2Fe_{12}P_7$, $Zr_6Ni_{20}P_{13}$, $Ho_5Ni_{19}P_{12}$, $Ho_{20}Ni_{66}P_{43}$, $(La,Ce)_{12}Rh_{30}P_{21}$, and $La_{18}Rh_{96}P_{51}$ (*1–9*). With the exception of the first three, all have hexagonal symmetry with a quite constant c axis close to 3.7 Å, a metal/nonmetal ratio equal or close to 2, and the same coordination polyhedra: lanthanoid (or Zr) in trigonal prismatic P coordination, transition metal (Ni, Fe, Rh) in pyramidal, tetrahedral, and triangular P coordination while phosphorus occupies a tricapped trigonal prism of metal atoms.

Such a structural homogeneity enables us to propose a new descriptive procedure using geometrical and crystallochemical principles and to establish a general classification scheme to describe and predict numerous structure types in pnictide, silicide, and also carbide chemistry.

This paper deals with the elaboration and the application of these principles.

II. Structural Features

In the course of our investigations of ternary lanthanoid–nickel (or rhodium)–phosphorus systems, we have prepared numerous compounds which crystallize in the following structure types: $Zr_2Fe_{12}P_7$, $Zr_6Ni_{20}P_{13}$, $(La,Ce)_{12}Rh_{30}P_{21}$, $Ho_{20}Ni_{66}P_{43}$, and $La_{18}Rh_{96}P_{51}$ (*5, 7–13*). Their main structural features are summarized in Table I. They

0022-4596/87 $3.00

TABLE I

MAIN STRUCTURAL FEATURES IN TERNARY LANTHANOID AND NICKEL (OR RHODIUM) PHOSPHIDES AND IN Fe_2P TYPE

	Fe_2P	$Ho_2Ni_{12}P_7$	$Ho_6Ni_{20}P_{13}$	$(La,Ce)_{12}Rh_{30}P_{21}$	$Ho_{20}Ni_{66}P_{43}$	$La_{18}Rh_{96}P_{51}$
Structure type	Fe_2P	$Zr_2Fe_{12}P_7$	$Zr_6Ni_{20}P_{13}$	$(La,Ce)_{12}Rh_{30}P_{21}$	$Ho_{20}Ni_{66}P_{43}$	$La_{18}Rh_{96}P_{51}$
a (Å)	5.865	9.063(1)	12.676(4)	17.475(3)	23.095(7)	27.054(6)
c (Å)	3.456	3.673(1)	3.730(2)	3.948(1)	3.742(4)	3.944(1)
V (Å^3)	102.95	261.3(1)	519.1(3)	1044.0(2)	1728.6(5)	2499.8(6)
Space group	$P\bar{6}2m$	$P\bar{6}$	$P6_3/m$	$P6_3/m$	$P6_3/m$	$P6_3/m$
Z	3	1	1	1	1	1
Sites						
tri.	—	—	2 Ni	6 Rh	6 Ni	6 Rh
tetr.	3 Fe	9 Ni	15 Ni	21 Rh	51 Ni	72 Rh
pyr.	3 Fe	3 Ni	3 Ni	3 Rh	9 Ni	18 Rh
6-prism.	—	2 Ho	6 Ho	12 Ln	20 Ho	18 La
Strongest reflection						
(n11) plane	111	211	311	411	611	711

all have hexagonal symmetry (Laue group $6/m$) with a regular increase of lattice volumes strongly depending on the a-axis. Moreover, the X-ray data show that the strongest reflection is attributed to the (n11) reticular plane: (211) for $Zr_2Fe_{12}P_7$, (311) for $Zr_6Ni_{20}P_{13}$, (411) for $(La,Ce)_{12}Rh_{30}P_{21}$, and so on.

These results lead us to propose that the $Zr_2Fe_{12}P_7$, $Zr_6Ni_{20}P_{13}$, $(La,Ce)_{12}Rh_{30}P_{21}$, $Ho_{20}Ni_{66}P_{43}$, and $La_{18}Rh_{96}P_{51}$ structure types in the same manner as the Fe_2P type (*14*) (Table I) are members of a structural series. The general chemical formula of the first members in this series may be written

$$A_{n(n-1)}B_{(n+1)(n+2)}C_{n(n+1)+1}. \qquad (1)$$

In relation (1), n is an integer and A, B, C correspond to lanthanoid (or Zr), transition metal (Fe, Ni, Rh), and phosphorus, respectively. Thus, when n is given the value 1, the composition B_6C_3 is obtained, which corresponds to the Fe_2P structure type ($Z = 3$). The members $n = 2$, 3, 4 are respectively the $Zr_2Fe_{12}P_7$, $Zr_6Ni_{20}P_{13}$, and $(La,Ce)_{12}Rh_{30}P_{21}$ structures. The unit cell parameter plot (Fig. 1) shows that the a axis increase obeys a linear law while the c axis is almost constant. By extrapolating the curves, the lattice constants of the AlB_2 structure are obtained ($a = 3.006$ Å, $c = 3.250$ Å) (*15*); nevertheless according to the electronegativity coefficients of aluminum and boron, the $n = 0$ member of our series should be the "Al_2B" structure (anti-AlB_2 type).

To describe and compare the structures, we have established a new descriptive system using triangular units in projection onto the (001) plane (Fig. 2). With the exception

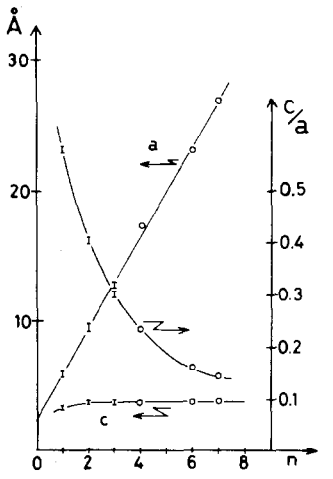

FIG. 1. Lattice constants plotted as a function of n for members of the series.

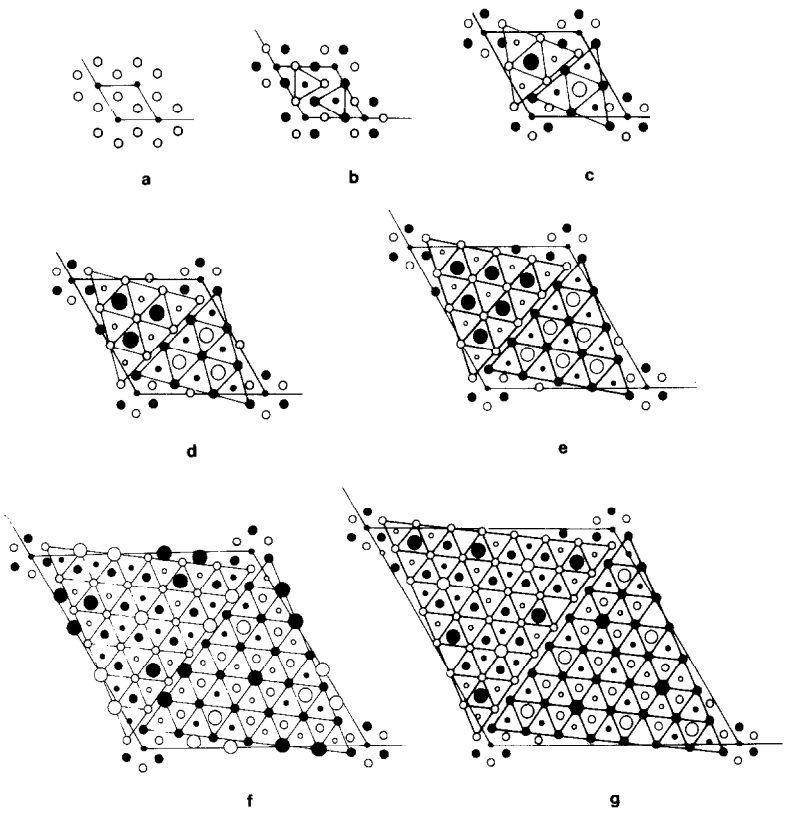

FIG. 2. Schematic representation of (a) anti-AlB_2, (b) Fe_2P, (c) $Zr_2Fe_{12}P_7$, (d) $Zr_6Ni_{20}P_{13}$, (e) $(La,Ce)_{12}Rh_{30}P_{21}$, (f) $Ho_{20}Ni_{66}P_{43}$, and (g) $La_{18}Rh_{96}P_{51}$ structures. Triangular units are emphasized. Large circles represent Zr, Ln atoms; medium circles, transition metal atoms (Fe, Ni, Rh); small circles, metalloid atoms. Black and white circles are separated from each other by one-half a period of the projection direction.

of the metalloid atom on the c axis, each hexagonal unit cell contains two equivalent triangular units, centered on threefold axes and mutually displaced by $c/2$. Each unit is in fact subdivided in n^2 simple triangles.

Figure 2 shows that the lengthening of the a axis strongly depends on the size of the triangular units. Since the c axis is quite invariant, the cell increase is therefore of two-dimensional type. A peculiar case is that of anti-AlB_2 type in which the unit consists of one B atom centered on the threefold axis.

Taking the structural results into account, i.e., A atoms in trigonal prismatic coordination of C atoms, B atoms either in pyramidal, tetrahedral, or triangular C coordination, and C atoms always in tricapped trigonal prisms of A and B atoms, the formula (1) may be put in the form

$$A^{6\text{-prism.}}_{n(n-1)}|B^{\text{pyr.}}_{5}B^{\text{tet.}}_{3(2n-1)}B^{\text{tri.}}_{(n-1)(n-2)}|C^{9\text{-prism.}}_{n(n+1)+1}.$$

The limiting composition to which the series converges is ABC with hexagonal symmetry and following coordinations $A^{6\text{-prism.}}B^{\text{tri.}}C^{9\text{-prism.}}$. Such a coordination scheme in hexagonal symmetry for A and B atoms has never been reported in the literature. Nevertheless, numerous hexagonal structures with ABC formula are mentioned (*16*) but

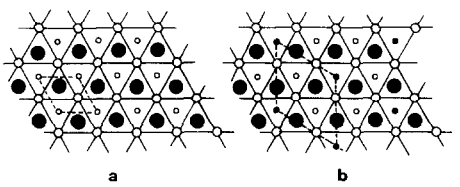

FIG. 3. Modes of representations of *ABC* compounds in hexagonal symmetry according to the coordination scheme: (a) $A^{6\text{-prism.}}\ B^{\text{tri.}}\ C^{9\text{-prism.}}$; (b) $A^{\text{pyr.}}\ B^{\text{tet.}}\ C^{9\text{-prism.}}$. Large, medium, and small circles correspond to *A*, *B*, and *C* atoms, respectively. Black and white circles are separated from each other by c/2. In case (b), metalloid sublattice displacement yields a larger unit cell with a threefold increase in volume.

the coordination scheme is then $A^{\text{pyr.}}B^{\text{tet.}}C^{9\text{-prism.}}$. A partial displacement of the metalloid sublattice explains the coordination exchange of metal atoms (Fig. 3) according to

$$|6\text{-prism.} + 3\text{-tri.}| \rightarrow |5\text{-pyr.} + 4\text{-tet.}|.$$

If the $A^{\text{pyr.}}\ B^{\text{tet.}}\ C^{9\text{-prism.}}$ distribution is observed in pnictide chemistry where *A* is a transition metal, for example, zirconium or niobium (ZrRuP, NbNiP) (*17, 18*), it has not yet been detected when *A* is a lanthanoid; indeed the smallest nonmetal coordination for a rare-earth metal is either trigonal prismatic or octahedral as in *Ln*P compounds of the rocksalt type (*19*).

As a consequence, when *A* is a lanthanoid, the formula (1) cannot be applied in the whole range $0 \leq n < \infty$ and has to be modified for higher *n* values to $(A,B)_{n(n-1)+(n+1)(n+2)}C_{n(n+1)+1}$. So, according to the coordination exchange, the number of *A* atoms in trigonal prisms and *B* atoms in triangles will decrease in favor of *B* atoms in pyramids and tetrahedra.

The first known example of coordination exchange is observed when *n* is given the value 6. According to formula (1), expected composition, for example, in the Ho–Ni–P system should be $Ho_{30}Ni_{56}P_{43}$ with the following coordination scheme $Ho_{30}^{6\text{-prism.}}|Ni_3^{\text{pyr.}}Ni_{33}^{\text{tet.}}Ni_{20}^{\text{tri.}}|P_{43}$. In fact, we have synthesized the compound $Ho_{20}Ni_{66}P_{43}$ corresponding to $Ho_{20}^{6\text{-prism.}}|Ni_9^{\text{pyr.}}Ni_{51}^{\text{tet.}}Ni_6^{\text{tri.}}|P_{43}$. An analogous result is also observed for the member $n = 7$.

As a consequence, the members $n = 6$ and 7 of our series exhibit more complicated triangular units; corresponding structures may be regarded as hybrids, built up by units of the $Zr_2Fe_{12}P_7$ and $Zr_6Ni_{20}P_{13}$ structures (Fig. 4).

Up to now, the term $n = 5$ has not yet been reported; its expected lattice parameters are $a \simeq 20$ Å and $c \simeq 3.70$ Å (Fig. 1). Two compositions for this term may be suggested: $A_{20}B_{42}C_{31}$ in accord with relation

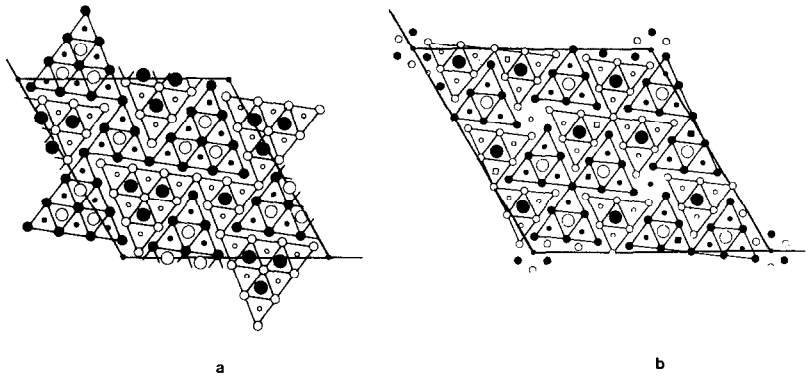

FIG. 4. Hybrid structures built up from $Zr_2Fe_{12}P_7$ and $Cr_6Ni_{20}P_{13}$ units of (a) $Ho_{20}Ni_{66}P_{43}$ and (b) $La_{18}Rh_{96}P_{51}$. For labeling of the atoms, see Fig. 2.

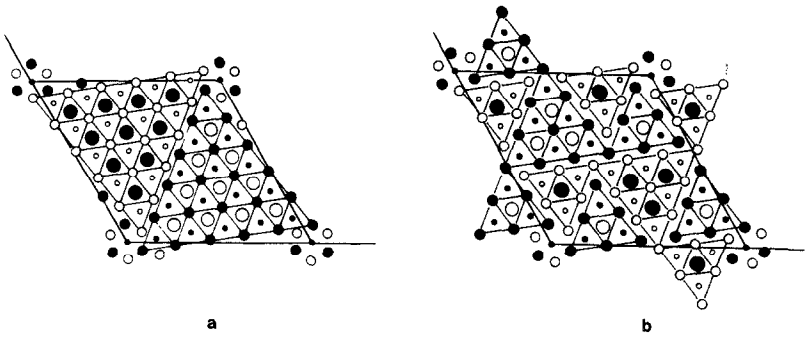

FIG. 5. Predicted structures of the member $n = 5$ of the series (a) $A_{20}B_{42}C_{31}$ (isolated units); (b) hybrid structure $A_{12}B_{50}C_{31}$. For labeling of the atoms, see Fig. 3.

(1), or $A_{12}B_{50}C_{31}$ if we take coordination exchange into account. In the latter case, the structure should appear as a hybrid, composed of $Zr_2Fe_{12}P_7$ and $Zr_6Ni_{20}P_{13}$ units (Fig. 5).

By plotting atomic percentages as a function of n, the most likely formula is $A_{20}B_{42}C_{31}$ (Fig. 6).

III. Descriptive Scheme Extension

As mentioned above, $Ho_{20}Ni_{66}P_{43}$ and $La_{18}Rh_{96}P_{51}$ structures are explained in terms of $Zr_2Fe_{12}P_7$ and $Zr_6Ni_{20}P_{13}$ units.

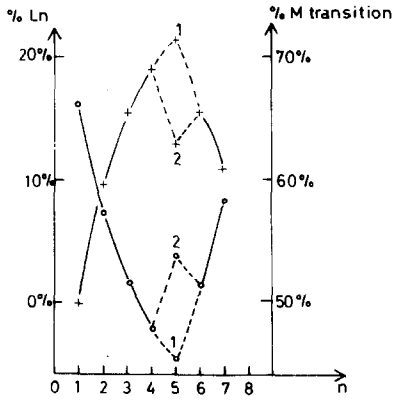

FIG. 6. Atomic percentages plotted as a function of n for members in the series. Circles and crosses correspond to transition metal and lanthanoid (or Zr) atomic percentages, respectively. (1) $A_{20}B_{42}C_{31}$, (2) $A_{12}B_{50}C_{31}$.

In a more general manner, numerous structures of pnictides, silicides and carbides may be described by a combination of units of anti-AlB_2, Fe_2P, $Zr_2Fe_{12}P_7$, $Zr_6Ni_{20}P_{13}$, and $(La,Ce)_{12}Rh_{30}P_{21}$ structure types. With reference to Fig. 7, these units will from now on be designated as (1:0), (3:1), (1:6:3), (3:10:6), and (6:15:10), respectively.

A combination of units into hybrid structures may be achieved in different ways.

A first mode of stacking consists of units of the same kind linked via a common vertex two by two in order to generate straight chains. Two neighboring chains are separated from each other by half a translation period of the projection direction.

As a example, the combination of (3:1) units (Fig. 8) shows the gradual symmetry change from hexagonal (isolated units) to

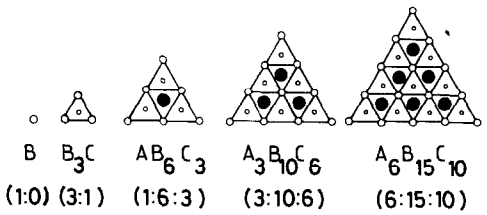

FIG. 7. Basic units of the classification scheme. Black and white circles are separated from each other by c/2. Large, medium, and small circles correspond to A, B, C atoms, respectively.

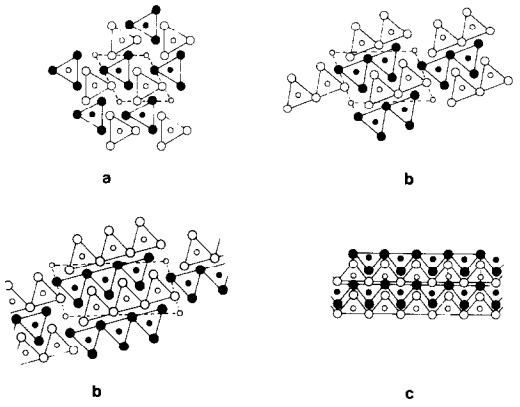

FIG. 8. Gradual symmetry change as a function of (3:1) combination units: (a) hexagonal, (b and c) monoclinic, (d) tetragonal symmetry.

tetragonal (infinite linear chains) via monoclinic symmetry (finite linear chains). The monoclinic angle gradually decreases from 120 to 90°.

One can easily extend this mode of stacking to (1:6:3), (3:10:6), even (6:15:10) units in order to generate at the ultimate step infinite straight chains. A somewhat different mode of stacking consists of infinite zigzag chains (Fig. 9).

An inventory of structural examples actually known can be divided into two groups:

(1) Structural examples with infinite linear chains are represented by Fe_2As (*20*), UNi_5Si_3 (*21*), and $HoCo_3P_2$ (*22*) which result from stacking of (3:1), (1:6:3), and (3:10:6) units, respectively. We shall call this group of structures the Fe_2As set (Fig. 10).

(2) Co_2P (*23*) and YCo_5P_3 (*24*) are the structural examples of infinite zigzag chains (shear after two units). We shall call this group the Co_2P set (Fig. 10).

The general chemical formula of members of both sets $A_{n(n-1)}B_{(n+1)(n+2)-2}C_{n(n+1)}$ results from relation (1). However, with the exception of odd terms of the Fe_2As set, the formula must be doubled for geometrical reasons (Table II).

A second type of combination consists of units of the same kind linked via a common vertex three at a time. All reported structures of binary and ternary compounds with such a stacking have hexagonal symmetry and exhibit vacancies. Indeed the common vertex that a metal atom should occupy in a triangular metalloid coordination is vacant (metal vacancy).

A combination of (1:6:3) units (Fig. 11a) may be used to describe the structures of ternary silicides of uranium and cobalt

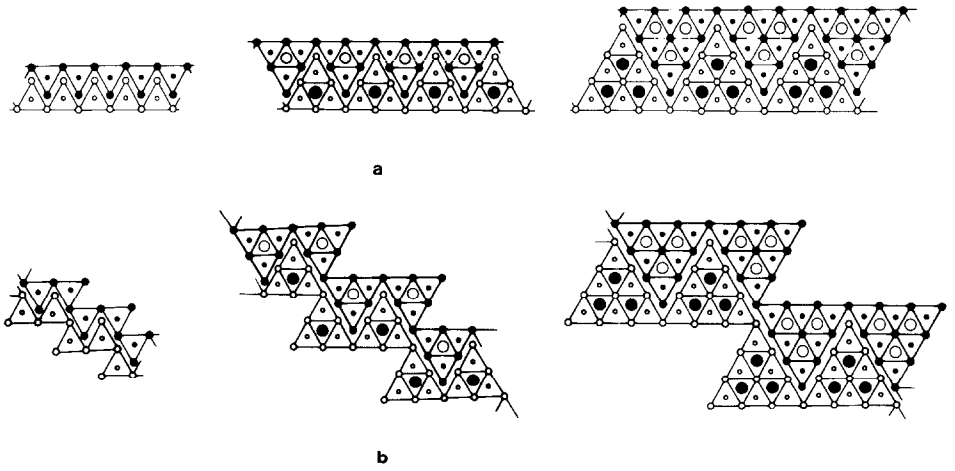

FIG. 9. Infinite linear (a) or zigzag (b) chains of (3:1), (1:6:3), or (3:10:6) units.

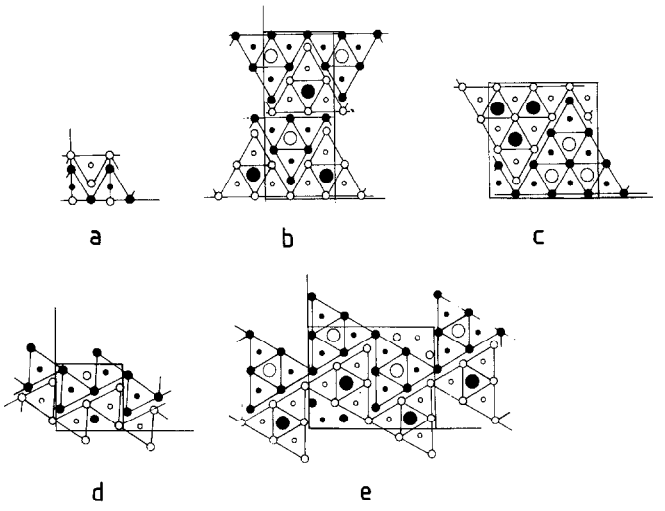

FIG. 10. Structural representations of (a) Fe_2As, (b) UNi_5Si_3, (c) $HoCo_3P_2$, (d) Co_2P, and (e) YCo_5P_3.

UCo_5Si_3 (*25*), $U_6Co_{30}Si_{19}$ (*26*), and $U_{10}Co_{51}Si_{33}$ (*27*). The structure of UCo_5Si_3 consists of "blocks" of three (1:6:3) units in a star-like arrangement. The structures of $U_6Co_{30}Si_{19}$ and $U_{10}Co_{51}Si_{33}$ are characterized by more complicated "blocks" of six and ten units, respectively (Fig. 11b). Each hexagonal unit cell contains two "blocks" mutually displaced from **c**/2.

TABLE II

MEMBERS IN THE Fe_2As AND Co_2P SETS

n	Predicted composition	Structural examples[a]
	(a) Fe_2As set	
1	B_4C_2	Fe_2As
2	$A_4B_{20}C_{12}$	UNi_5Si_3
3	$A_6B_{18}C_{12}$	$HoCo_3P_2$
4	$A_{24}B_{56}C_{40}$	"$A_3B_7C_5$"
	(b) Co_2P set	
1	B_8C_4	Co_2P
2	$A_4B_{20}C_{12}$	YCo_5P_3
3	$A_{12}B_{36}C_{24}$	"AB_3C_2"
4	$A_{24}B_{56}C_{40}$	"$A_3B_7C_5$"

[a] Structural examples not yet reported are in quotation marks.

By stacking more than three units ($U_6Co_{30}Si_{19}$ and $U_{10}Co_{51}Si_{33}$) triangular channels within "blocks" occur into which (3:1) units are inserted (Fig. 11). The ultimate step of combination yields the limiting composition $\square AB_6C_4$, the structure of which is built up from one (1:6:3) and one (3:1) unit (Fig. 12). Up to now, no structural example with such a stacking is known.

The general chemical formula of members in this series is $\square_{n(n-1)}A_{n(n+1)}B_{6(n^2+1)}C_{2(2n^2+1)}$ (Table III).

When *n* is given the value 1, the chemical formula is $A_2B_{12}C_6$, close to that of $A_2B_{12}C_7$

TABLE III

MEMBERS IN THE SERIES $\square_{n(n-1)}A_{n(n+1)}B_{6(n^2+1)}C_{2(2n^2+1)}$

n	Predicted composition	Structural examples
1	$\square_0A_2B_{12}C_6$	"$A_2B_{12}C_6$"
2	$\square_2A_6B_{30}C_{18}$	UCo_5Si_3
3	$\square_6A_{12}B_{60}C_{38}$	$U_6Co_{30}Si_{19}$
4	$\square_{12}A_{20}B_{102}C_{66}$	$U_{10}Co_{51}Si_{33}$
5	$\square_{20}A_{30}B_{156}C_{102}$	"$A_{10}B_{52}C_{34}$"
⋮		
∞	$\square AB_6C_4$	"AB_6C_4"

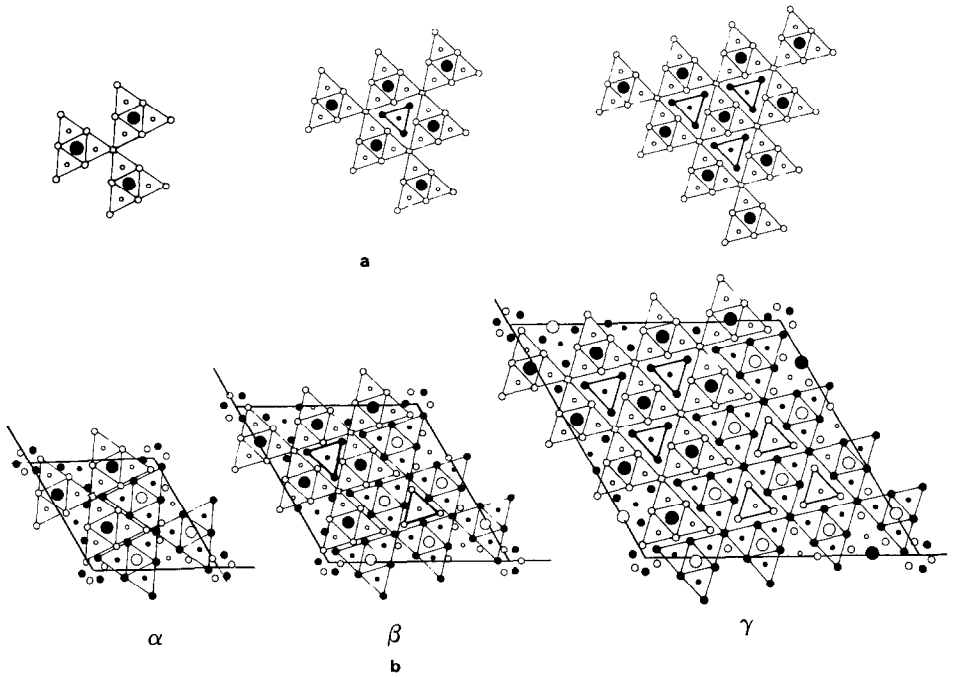

FIG. 11. (a) Progressive stacking of (1:6:3) units as "blocks" via common vertices. The inserted (3:1) units are emphasized. (b) Structural representation of (α) UCo_5Si_3, (β) $U_6Co_{30}Si_{19}$, and (γ) $U_{10}Co_{51}Si_{33}$.

($Zr_2Fe_{12}P_7$ type). The only difference results from a metalloid vacancy on the c axis in the silicides; we shall call this group of structures the $Zr_2Fe_{12}P_7$ set.

Identical combination of (3:1) units yields a series of defective binary compounds. The structures of $Cr_{12}P_7$ (*28*), $Rh_{20}Si_{13}$ (*29*), and hypothetical "$B_{30}C_{21}$" are respectively the first, second, and third steps of this stacking (Fig. 13). By joining more than three (3:1) units ($Rh_{20}Si_{13}$ and "$B_{30}C_{21}$"), there appear triangular voids into which (1:0) units are inserted. The limiting composition to which the series converges is $\square BC$ (Table IV) which is that of tungsten carbide WC (*30*) (Fig. 12).

The chemical formula of the structural members in this series $\square_{n(n-1)}B_{(n+1)(n+2)}C_{n(n+1)+1}$ is closely related to formula (1)

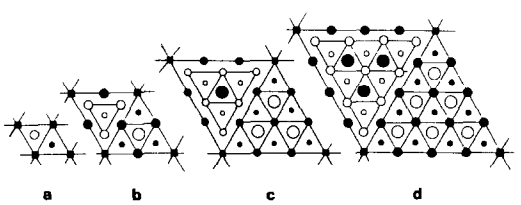

FIG. 12. Structural representation of limiting members resulting from combination three at a time of units (a) WC, (b) "AB_6C_4," (c) $Zr_4Co_{13}Si_9$, (d) "$A_9B_{22}C_{16}$."

TABLE IV

MEMBERS IN THE BINARY SERIES $\square_{n(n-1)}B_{n(n+1)(n+2)}C_{n(n+1)+1}$

n	Predicted composition	Structural examples
1	$\square_0B_6C_3$	Fe_2P
2	$\square_2B_{12}C_7$	$Cr_{12}P_7$
3	$\square_6B_{20}C_{13}$	$Rh_{20}Si_{13}$
4	$\square_{12}B_{30}C_{21}$	"$B_{30}C_{21}$"
5	$\square_{20}B_{42}C_{31}$	"$B_{42}C_{31}$"
⋮		
∞	$\square BC$	WC

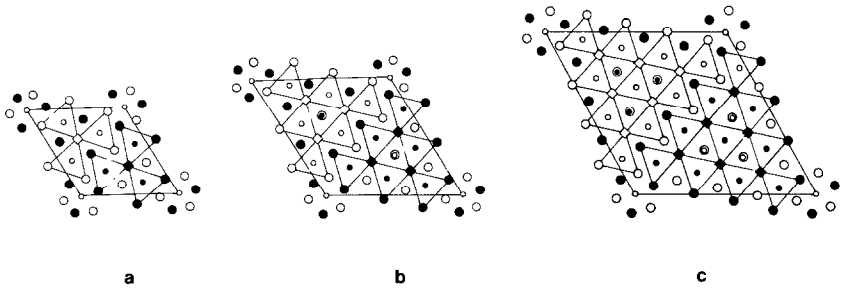

FIG. 13. Combination of (3:1) units three at a time: (a) $Cr_{12}P_7$, (b) $Rh_{20}Si_{13}$, and (c) "$B_{30}C_{21}$." Double circles indicate inserted (1:0) units.

$A_{n(n-1)}B_{(n+1)(n+2)}C_{n(n+1)+1}$ when considering A as a vacancy. Thus $Cr_{12}P_7$, $Rh_{20}Si_{13}$, and "$B_{30}C_{21}$" structures may be regarded as unfilled $Zr_2Fe_{12}P_7$, $Zr_6Ni_{20}P_{13}$, and $(La,Ce)_{12}Rh_{30}P_{21}$ ones.

In the same manner, the combination of three at a time via a common vertex of (3:10:6) or (6:15:10) units leads to more complicated networks. The stacking of (3:10:6) units results in triangular voids into which (1:6:3) units are placed. Another series of defective ternary compounds is then obtained with the general formula $\square_{n(n-1)}A_{2(2n^2+1)}B_{13n^2-5n+12}C_{9n^2-3n+6}$ (Table V).

So far, no structural examples of intermediate steps have been reported; only the limiting composition $\square A_4B_{13}C_9$ is known which is the structure of ternary silicide of zirconium and cobalt $Zr_4Co_{13}Si_9$ (*27*) (Fig. 12).

TABLE V

MEMBERS IN THE SERIES $\square_{n(n-1)}A_{2(2n^2+1)}B_{13n^2-5n+12}C_{9n^2-3n+6}$

n	Predicted composition	Structural examples
1	$\square_0A_6B_{20}C_{12}$	"$A_6B_{20}C_{12}$"
2	$\square_2A_{18}B_{54}C_{36}$	"AB_3C_2"
3	$\square_6A_{38}B_{114}C_{78}$	"$A_{19}B_{57}C_{39}$"
4	$\square_{12}A_{66}B_{200}C_{138}$	"$A_{33}B_{100}C_{69}$"
5	$\square_{20}A_{102}B_{312}C_{216}$	"$A_{17}B_{52}C_{36}$"
⋮		
∞	$\square A_4B_{13}C_9$	$Zr_4Co_{13}Si_9$

No example is known of stacking of (6:15:10) with insered (3:10:6) units. Predicted compositions in this series obey the general formula $\square_{n(n-1)}A_{9n^2-3n+6}B_{22n^2-12n+20}C_{16n^2-8n+12}$ with limiting formula $\square A_9B_{22}C_{16}$ (Fig. 12).

Other peculiar modes of combination may also describe hybrid structures. Examples are the structures of $Ho_{20}Ni_{66}P_{43}$ and $La_{18}Rh_{96}P_{51}$ discussed previously. Other examples can be found in pnictide and silicide chemistry. To illustrate these peculiar modes of combination, the structures of the two phosphides, $Ho_5Ni_{19}P_{12}$ (*6*) and $Hf_8Co_{16}P_{12}$ (*31*), and the silicide, $U_9Co_{37}Si_{25}$ (*27*), will now be discussed (Fig. 14).

The first one consists of (1:6:3) and (3:10:6) units in the ratio 2 : 1. The (1:6:3) units share common vertices to generate triangular channels, located around the c axis of the hexagonal structure, into which the (3:10:6) units are inserted.

In the second one, the total framework resembles $Ho_5Ni_{19}P_{12}$; however, the (3:10:6) unit is somewhat different since, in contrast to rare-earth elements, hafnium atoms occupy both trigonal prismatic and pyramidal phosphorus sites in the structure.

A more complicated stacking is that in the ternary silicide of uranium and cobalt $U_9Co_{37}Si_{25}$ in which (3:1), (1:6:3), and (3:10:6) units occur simultaneously. The (3:10:6) and (1:6:3) units are linked together to form channels which are occupied either

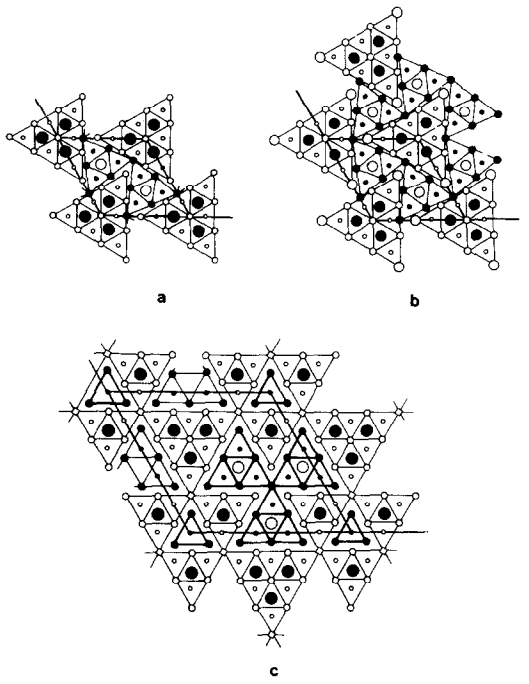

FIG. 14. Peculiar modes of combination: (a) $Ho_5Ni_{19}P_{12}$, (b) $Hf_2Co_4P_3$, and (c) $U_9Co_{37}Si_{25}$.

by "blocks" of three units as in UCo_5Si_3 type or by isolated (3:1) units located around the c axis.

Conclusion

We have proposed a new classification scheme built up by triangular units which occur in five basic structures: anti-AlB_2, Fe_2P, $Zr_2Fe_{12}P_7$, $Zr_6Ni_{20}P_{13}$, and $(La,Ce)_{12}Rh_{30}P_{21}$. Various modes of stacking of the units enable us to clearly describe and classify known structures. Moreover, our method may serve as a powerful tool for predicting new structures since several series of chemical formulations have been established. Finally, as summarized in Fig. 15, the method permits the correlation of a great number of structure types in pnictide, silicide, and even carbide chemistry.

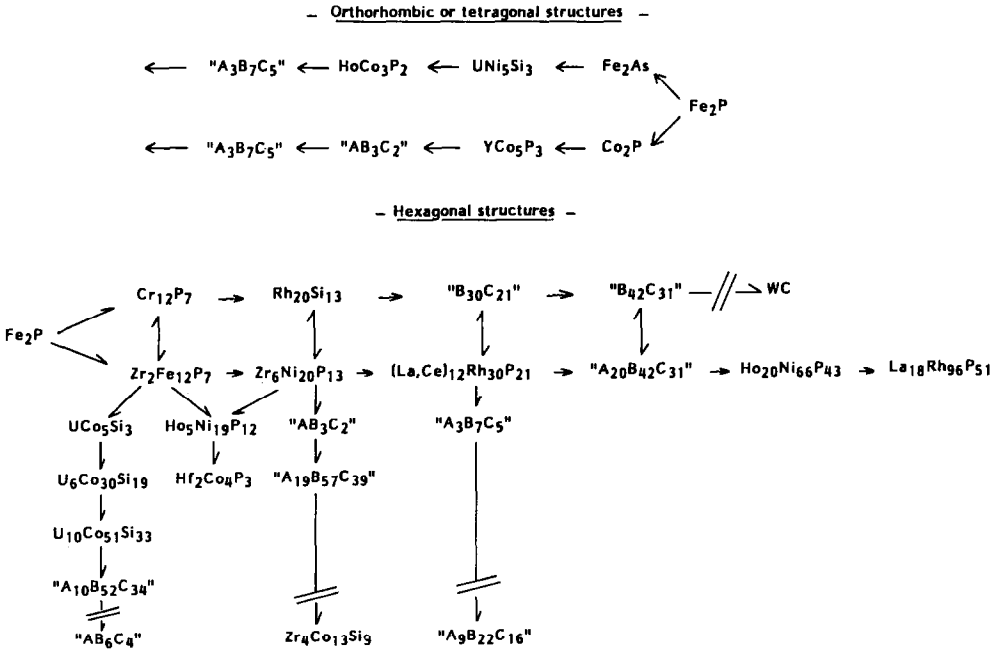

FIG. 15. Structural relationship resulting from our classification in pnictide, silicide, and carbide chemistry.

References

1. Z. Ban and M. Sikirica, *Acta Crystallogr.* **18,** 594 (1965).
2. D. J. Braun and W. Jeitschko, *Acta Crystallogr. Sect. B* **34,** 2069 (1978).
3. V. N. Davydov and Yu. B. Kuz'ma, *Dopov Akad Nauk. Ukr. RSR, ser. A: Fiz. Mat. Tekh. Nauk.* **1,** 82 (1981).
4. E. Ganglberger, *Monatsh. Chem.* **99,** 557 (1968).
5. R. Guérin, E. H. El Ghadraoui, J. Y. Pivan, J. Padiou, and M. Sergent, *Mat. Res. Bull.* **19,** 1257 (1984).
6. J. Y. Pivan, R. Guérin, and M. Sergent, *Inorg. Chem. Acta* **109,** 3, 221 (1985).
7. J. Y. Pivan, R. Guérin, and M. Sergent, *Mat. Res. Bull.* **20,** 887 (1985).
8. J. Y. Pivan and R. Guérin, *J. Less Common Met.*, **120,** 247 (1986).
9. J. Y. Pivan, Thèse d'Université, University of Rennes, France, 1985.
10. J. Y. Pivan, R. Guérin, and M. Sergent, *C.R. Acad. Sci. Paris* **299,** 9, 553 (1984).
11. J. Y. Pivan, R. Guérin, and M. Sergent, *C.R. Acad. Sci. Paris* **299,** 11, 689 (1984).
12. J. Y. Pivan, R. Guérin, and M. Sergent, *J. Less Common Met.* **107,** 249 (1985).
13. J. Y. Pivan, R. Guérin, J. Padiou, and M. Sergent, *J. Less Common Met.* **118,** 2, 191 (1986).
14. S. Rundqvist and F. Jellinek, *Acta Chem. Scand.* **13,** 425 (1959).
15. W. Hofmann and W. Janische, *Z. Phys. Chem. B* **31,** 214 (1936).
16. R. Fruchart, *Ann. Chim.* **7,** 563 (1982).
17. H. Barz, H. C. Ku, G. P. Meisner, Z. Fisk, and B. T. Matthias, *Proc. Natl. Acad. Sci. USA* **77,** 3132 (1980).
18. S. Rundqvist and P. Tansuriwong, *Acta Chem. Scand.* **21,** 813 (1967).
19. A. Iandelli and E. Botti, *Atti Reale Accad. Nazl. Lincei* **24,** 459 (1936).
20. M. Elander, G. Hägg, and A. Westgren, *Ark. Kem. Mineral. Geol. B* **12,** 1 (1936).
21. L. G. Aksel'rud, V. I. Yarovets, O. I. Bodak, Ya. P. Yarmolyuk, and E. I. Gladyshevskii, *Sov. Phys. Kristallogr.* **21,** 210 (1976).
22. W. Jeitschko and U. Jakubowski, *J. Less Common Met.* **110,** 339 (1985).
23. S. Rundqvist, *Acta Chem. Scand.* **14,** 1961 (1960).
24. U. Meisen and W. Jeitschko, *J. Less Common Met.* **102,** 127 (1984).
25. Ya. P. Yarmolyuk, L. G. Aksel'rud, and E. I. Gladyshevskii, *Kristallografiya* **23,** 942 (1978).
26. Ya. P. Yarmolyuk, L. G. Aksel'rud, V. S. Fundamenskii, and E. I. Gladyshevskii, *Sov. Phys. Kristallogr.* **25,** 1, 97 (1980).
27. E. I. Gladyshevskii and Yu. N. Grin', *Sov. Phys. Kristallogr.* **26,** 6, 683 (1981).
28. H. K. Chun and G. B. Carpenter, *Acta Crystallogr. Sect. B* **35,** 30 (1979).
29. I. Engström, *Acta Chem. Scand.* **19,** 1924 (1965).
30. E. Parthé and V. Sadagopan, *Monatsh. Chem.* **93,** 263 (1962).
31. E. Ganglberger, *Monatsh. Chem.* **99,** 566 (1968).